

Biomimetic synthesis of calcium carbonate with different morphologies under the direction of different amino acids

Yuming Guo · Feifei Wang · Jie Zhang · Lin Yang · Xiaoman Shi · Qilong Fang · Xiaoming Ma

Received: 7 June 2012 / Accepted: 7 August 2012 / Published online: 21 August 2012
© Springer Science+Business Media B.V. 2012

Abstract Using three different amino acids (AAs) as organic matrices, including the highly nonpolar hydrophobic L-valine, the positively charged L-arginine and the less polar uncharged L-serine, calcium carbonate (CaCO_3) with different morphologies and polymorphs were synthesized by a facile gas diffusion reaction based on biomimetic strategy. Compared with the control cubic calcite obtained in the absence of AAs, the product from L-valine was cubic calcite aggregates assembled by nano-platelets. The product from L-arginine was spherical vaterite aggregates assembled by spherical nanoparticles. The product from L-serine was the mixture of cubic calcite and spherical vaterite. The structures and properties of the side chains of the AAs exerted the significant effects on the nucleation and growth of the CaCO_3 . The formation mechanisms of the CaCO_3 in the presence of AAs are preliminarily discussed. The results suggest that the polymorphs and morphologies of the inorganic nanomaterials might be easily adjusted through the careful selection of the organic matrices.

Keywords Biomimetic · CaCO_3 · Amino acids · Morphologies · Crystal growth

Introduction

Biominerals are the inorganic phase formed in biological systems and widespread in nature. The biominerals exhibit special hierarchical structures and important

Y. Guo (✉) · F. Wang · J. Zhang · L. Yang (✉) · X. Shi · Q. Fang · X. Ma
College of Chemistry and Chemical Engineering, Engineering Technology Research Center of Motive Power and Key Materials of Henan Province, Henan Normal University, Xinxiang 453007, People's Republic of China
e-mail: guoyuming@gmail.com

L. Yang
e-mail: yanglin1819@163.com

biological functions, such as the silica cell wall of the marine diatom, the calcitic spine of the sea urchin, and the calcitic coccolith of the marine algae [1–8]. The processes that lead to the formation of the biominerals are called biomineralization. Based on biomineralization research, novel synthetic methods have been constructed, i.e. biomimetic synthesis. Through the biomimetic synthesis, the crystal morphologies, polymorphs, and properties can be easily adjusted. Therefore, the biomimetic preparation of the inorganic micro/nano-crystals with specific structures has attracted tremendous attention, and great efforts have been made to prepare these structures [9–13]. However, most of the existing methods frequently involve rigorous experimental conditions, such as high temperature and high pressure, which severely limit the corresponding practical applications.

As one of the important biominerals frequently found in mammalian hard tissues, calcium carbonate (CaCO_3) exhibits considerable potential applications in various fields including drug delivery and ion adsorption/exchange owing to its unique properties, e.g., the biocompatibility, biodegradability, and pH sensitivity [11, 14, 15]. Therefore, the facile synthesis of CaCO_3 with specific structures has attracted tremendous attention. As the building units of proteins, amino acids (AAs) have amino and carboxyl groups simultaneously. AAs can regulate the nucleation, growth, and structures of the inorganic crystals to a certain extent through the coordination interactions between AAs and metal ions [16–20]. However, reports on the regulation mechanism of different kinds of AAs on the biomimetic synthesis of CaCO_3 with specific structures are rare and attract great interest. In the present study, using three different kinds of AAs as organic matrices, namely the highly nonpolar hydrophobic L-valine, the positively charged L-arginine, and the less polar uncharged L-serine, different morphologies and polymorphs of CaCO_3 were successfully prepared by a facile gas diffusion reaction based on a biomimetic strategy. Based on the results, the regulation mechanisms of the AAs on the CaCO_3 formation are also proposed.

Materials and methods

Calcium chloride (CaCl_2), sodium carbonate (Na_2CO_3), L-valine, L-arginine, and L-serine were purchased from China National Pharmaceutical Group. All the chemicals used in this study were of analytical grade and were used as received without further purification. Double-distilled water (DD water) was used in all the experiments.

Firstly, the fresh CaCO_3 precipitate was prepared as follows: 100 mL of 0.5 M CaCl_2 solution was mixed with 100 mL of 0.5 M Na_2CO_3 solution under moderate stirring and incubated for 6 h at room temperature. The precipitate was collected by centrifugation and washed several times with DD water and absolute ethanol. The obtained product was dried under vacuum for 24 h at 40 °C and denoted as fresh CaCO_3 .

The fresh CaCO_3 precipitate was suspended into DD water under vigorous stirring. Then, the suspension was bubbled with high-purity CO_2 gas under moderate stirring for 12 h and centrifuged to remove any remained precipitate to

prepare the saturated $\text{Ca}(\text{HCO}_3)_2$ aqueous solution. Subsequently, AAs/ $\text{Ca}(\text{HCO}_3)_2$ aqueous solutions with different concentrations of AAs (1, 10, 50 mM) were prepared using the saturated $\text{Ca}(\text{HCO}_3)_2$ aqueous solution as the solvent. The mole ratios of AAs to Ca^{2+} are 1:10, 1:1, and 5:1, respectively. The AAs/ $\text{Ca}(\text{HCO}_3)_2$ aqueous solutions were sealed and stirred for 6 h to allow the complete interaction between the Ca^{2+} and the AAs. Then, beakers containing 25 mL of AAs/ $\text{Ca}(\text{HCO}_3)_2$ were covered with Parafilm punched with pinholes and placed into a desiccator. Another beaker containing 10 mL of ammonia liquor was also covered with Parafilm punched with pinholes and placed at the bottom of the same desiccator. Because of the increase of the pH value of the aqueous solutions of the AAs/ $\text{Ca}(\text{HCO}_3)_2$ through the gradual diffusion of ammonia, CaCO_3 was gradually formed. After reacting for 7 days, the products were collected by centrifugation and washed several times with DD water and absolute ethanol. The obtained products were dried under vacuum for 24 h at 40 °C and denoted as valine- CaCO_3 , arginine- CaCO_3 , and serine- CaCO_3 . For comparison, a control experiment was performed to prepare bulk CaCO_3 in the absence of AAs under similar conditions.

The size and morphology of the products were determined by scanning electron microscopy (SEM; JEOL JSM-6390LV). The powder X-ray diffraction (XRD) patterns were recorded on a Bruker AXS D8Advance X-ray diffractometer with graphite monochromatized $\text{Cu K}\alpha$ radiation ($\lambda = 0.15406$ nm) in the 2θ range of 20–70°. The Fourier transform infrared spectroscopy (FT-IR) spectra of the products were recorded on a Bio-Rad FTS-40 Fourier transform infrared spectrometer in the wavenumber range of 4,000–400 cm^{-1} .

Results and discussion

In the present study, the biomimetic synthesis of the CaCO_3 was accomplished in two steps. In the first step, the Ca^{2+} -AAs complex were formed through the coordination interactions between the AAs and the Ca^{2+} . In the second step, the CaCO_3 with specific hierarchical three-dimensional structures was formed with the increase of the pH value through the dissolution of the ammonia into the coordination system (Eqs. 1, 2).

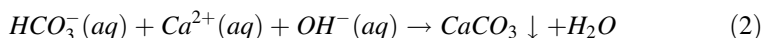
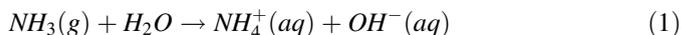


Figure 1 shows the SEM images of the as-prepared valine- CaCO_3 in the presence of the different concentrations of L-valine aqueous solution. In the Figure, in the presence of the 1 and 10 mM aqueous solutions of L-valine, the as-prepared CaCO_3 are the large particles with irregular morphologies (Fig. 1a, b). However, when the concentration of the L-valine is increased to 50 mM, the as-prepared CaCO_3 are the well-dispersed cubic-like assemblies with average side length of 6.58 μm and narrow size distribution (Fig. 1c). From the magnified SEM image (Fig. 1d), the cubic assemblies are assembled by the platelets with the nanoscale thickness and average side length of 2.73 μm .

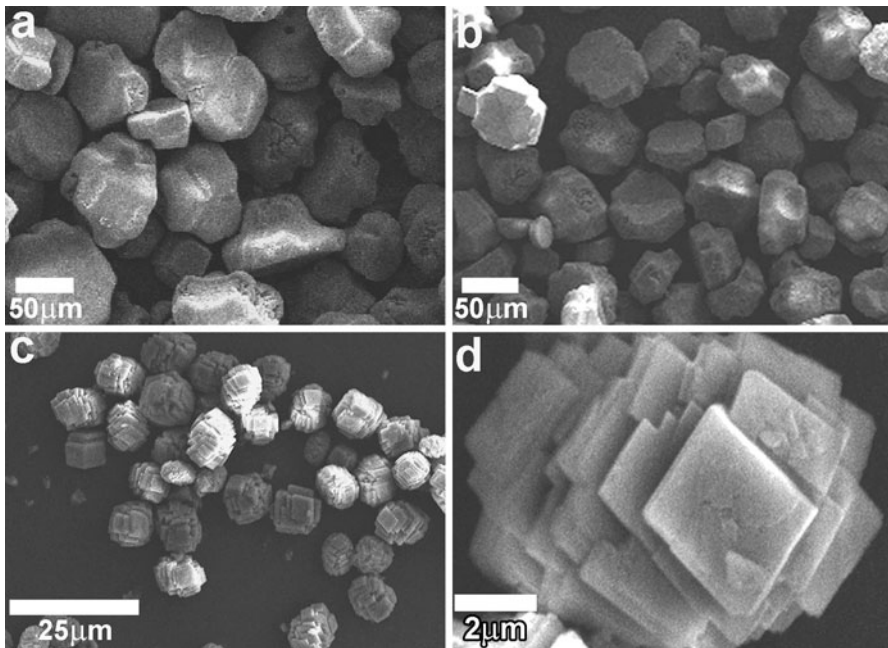


Fig. 1 SEM images of the CaCO_3 prepared in the presence of the different concentrations of L-valine aqueous solution. **a** 1 mM, **b** 10 mM, **c** 50 mM, **d** magnified SEM image of (c)

Figure 2 shows the SEM images of the as-prepared arginine- CaCO_3 in the presence of the different concentrations of L-arginine aqueous solution. In the Figure, in the presence of the 1 mM aqueous solution of L-arginine, the as-prepared CaCO_3 is the big ellipsoid with average diameter of 25 μm (Fig. 2a). In the presence of the 10 mM aqueous solution of L-arginine, the as-prepared CaCO_3 is the mixture of microspheres and cubes (Fig. 2b). However, when the concentration of the L-arginine is increased to 50 mM, the as-prepared CaCO_3 are the well-dispersed microspheres with average diameter of 11.42 μm and narrow size distribution (Fig. 2c). From the magnified SEM image of a single sphere (Fig. 2d), it can be seen to be composed of a large number of nanoparticles.

Figure 3 shows the SEM images of the as-prepared arginine- CaCO_3 prepared in the presence of the different concentrations of L-serine aqueous solution. In the Figure, in the presence of the 1 mM aqueous solution of L-serine, the as-prepared CaCO_3 are the big particles with irregular morphologies (Fig. 3a). In the presence of the 10 mM aqueous solution of L-serine, the as-prepared CaCO_3 is the mixture of microspheres and cubes (Fig. 3b). When the concentration of the L-serine is increased to 50 mM, the as-prepared CaCO_3 are composed of two different morphologies, the hollow microspheres and the cube-like crystals (Fig. 3c, d).

However, from Fig. 4, the bulk CaCO_3 obtained from the control experiment in the absence of the AAs are the large cubic crystals with average side length of about 34.3 μm and wide size distribution, significantly different from the CaCO_3 prepared in the presence of the AAs. From these results, the presence of the AAs is an

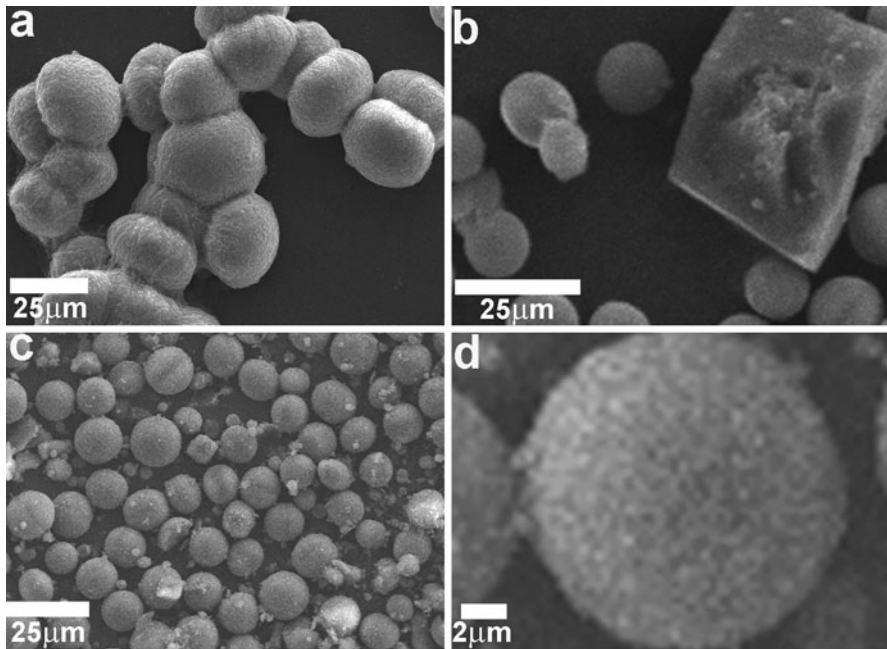


Fig. 2 SEM images of the CaCO_3 prepared in the presence of the different concentrations of L-arginine aqueous solution. **a** 1 mM, **b** 10 mM, **c** 50 mM, **d** magnified SEM image of (c)

important factor for the successful preparation of the well-dispersed CaCO_3 . Furthermore, the morphologies of the as-prepared CaCO_3 can be adjusted through the careful selection of the structures and concentrations of the AAs.

Figure 5 presents the XRD patterns of the as-prepared valine- CaCO_3 , serine- CaCO_3 , arginine- CaCO_3 , and bulk CaCO_3 , respectively. In the Figure, the valine- CaCO_3 exhibit identical diffraction peaks to the calcite (PDF 83-0578), indicating the successful preparation of the calcite under the direction of the valine. The XRD pattern of the arginine- CaCO_3 presents the identical diffraction peaks to the vaterite (PDF 33-0268), revealing the successful preparation of vaterite under the direction of arginine. For the CaCO_3 prepared under the direction of the serine, the diffraction peaks can be assigned to vaterite and calcite, indicating the presence of these two polymorphs in the serine- CaCO_3 . In the serine- CaCO_3 , the hollow microspheres might be the vaterite, and the cube-like crystals might be the calcite. From the XRD pattern of the bulk CaCO_3 prepared in the absence of AAs, the bulk CaCO_3 is the calcite (PDF 83-0578).

In order to further confirm the polymorphs of the as-prepared products in the presence of different AAs, the valine- CaCO_3 , arginine- CaCO_3 , and serine- CaCO_3 are characterized by FT-IR spectroscopy and the corresponding results are shown in Fig. 6. In the Figure, the FT-IR spectrum of the valine- CaCO_3 exhibits the characteristic bands of calcite at 712 and 875 cm^{-1} [21], confirming the formation of calcite in the presence of valine. The presence of the characteristic bands of vaterite at 745, 876, and 1,088 cm^{-1} in the spectrum of the arginine- CaCO_3 reveals

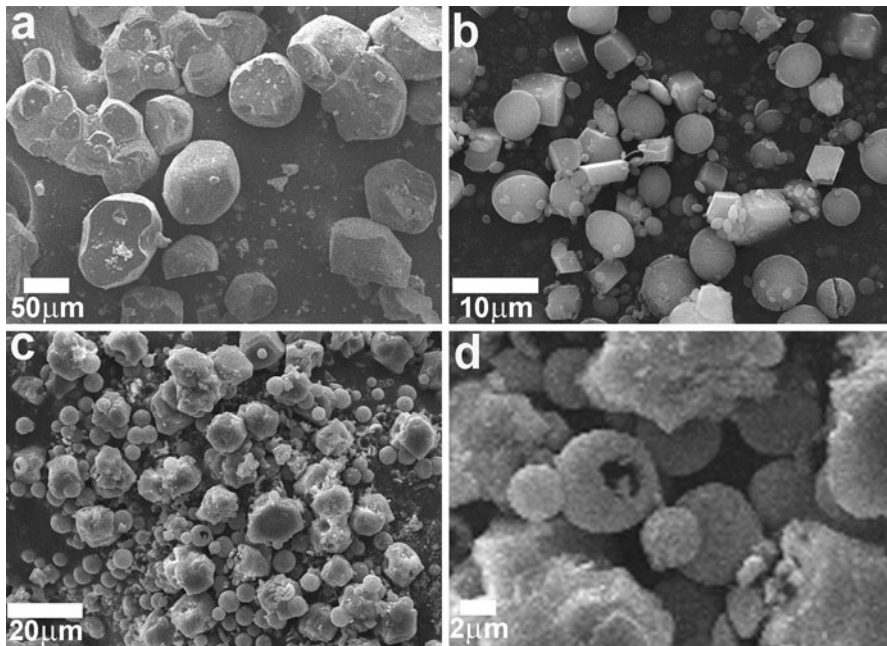


Fig. 3 SEM images of the CaCO_3 prepared in the presence of the different concentrations of L-serine aqueous solution. **a** 1 mM, **b** 10 mM, **c** 50 mM, **d** magnified SEM image of (c)

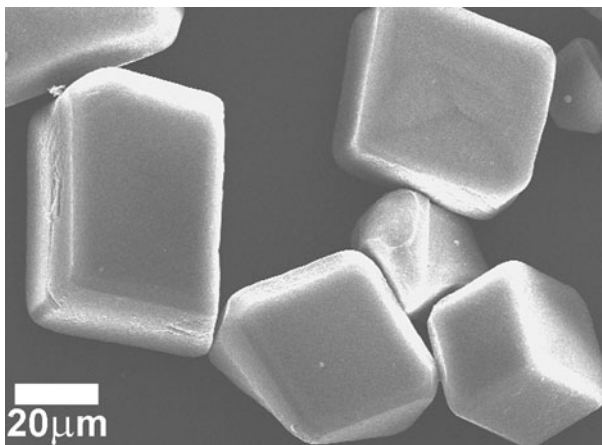


Fig. 4 SEM image of the bulk CaCO_3 prepared in the absence of the AAs

the formation of vaterite under the direction of arginine [22]. Similarly, the simultaneous formation of vaterite and calcite in the presence of serine is also confirmed according to the characteristic bands of calcite at 712 and 875 cm^{-1} and vaterite at 745 and $1,088\text{ cm}^{-1}$ in the spectrum of the serine- CaCO_3 .

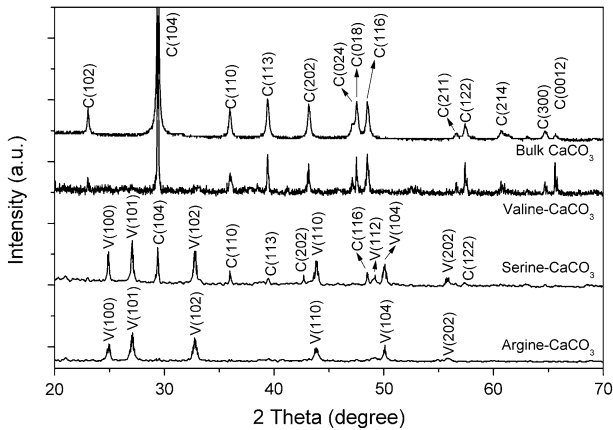


Fig. 5 XRD patterns of the as-prepared valine- CaCO_3 , serine- CaCO_3 , and arginine- CaCO_3 . The capital letter *C* represents the diffraction peaks of calcite; *V* represents the diffraction peaks of vaterite

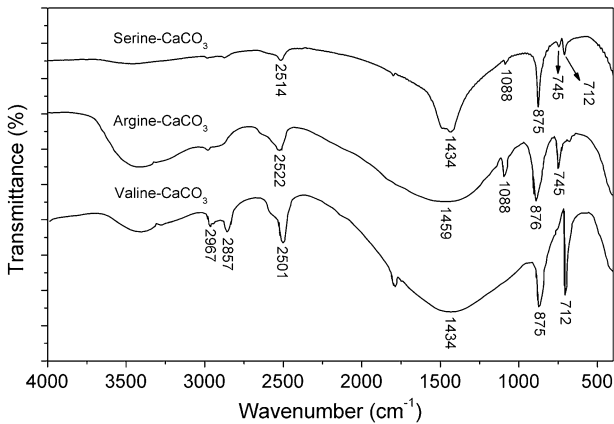


Fig. 6 FT-IR spectra of the as-prepared valine- CaCO_3 , arginine- CaCO_3 , and serine- CaCO_3

Based on the results, formation mechanisms of the as-prepared products are proposed (Fig. 7). According to the structures, the valine, arginine, and serine are classified as the highly nonpolar hydrophobic, positively charged, and less polar uncharged AA at physiological pH, respectively. Under the neutral pH condition, the hydrophobic side chain of the valine cannot interact with the calcium ions (Ca^{2+}) and hydrocarbonate ions (HCO_3^-) at the beginning of the reaction and cannot affect the nucleation. This results in the formation of the crystal seed of calcite, the most stable polymorph of CaCO_3 . With the proceeding of the reaction, the pH of the system gradually increased, leading to the increase of the concentration of the anion form. The anion form of the valine can interact with Ca^{2+} and affect the growth of the crystals, resulting in the formation of the cubic aggregates. For the positively charged arginine, there is strong electrostatic

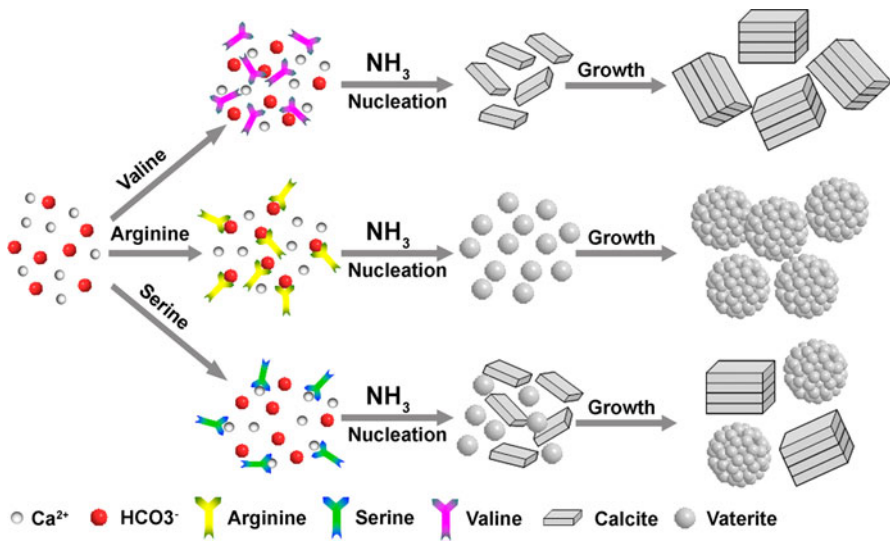


Fig. 7 Possible formation mechanisms of the as-prepared CaCO₃ in the presence of different AAs

interaction between the positive charged side chain of the arginine and the HCO₃⁻ to form the stable complex, which will affect the nucleation of the CaCO₃ to form the vaterite. For the less polar uncharged serine, there is moderate electrostatic interaction between the polar side chain of the serine and Ca²⁺. Some of the Ca²⁺ will form the complex with the serine; the others remain the free ions. This results in the simultaneous nucleation of calcite and vaterite to form the two polymorphs.

Conclusions

In summary, using three different AAs including L-valine, L-serine, and L-arginine as organic matrices, CaCO₃ with different polymorphs and morphologies were successfully prepared through a facile gas diffusion method based on a biomimetic strategy. The structures and properties of the side chains of the AAs exerted significant effects on the nucleation and growth of the CaCO₃. This suggests that the polymorphs and morphologies of the inorganic nanomaterials might be easily adjusted through the careful selection of the molecular structures of the organic matrices. More importantly, based on this idea, the inorganic nanomaterials with special structures and properties might be successfully prepared through the modification of the molecular structures of the organic matrices.

Acknowledgments This work was financially supported by the National Science Foundation of China (21171051, 21271066) and the Program for Changjiang Scholars and Innovative Research Team in University (IRT1061) and the Innovation Fund for Outstanding Scholar of Henan Province (114200510004) and Henan Key Proposed Program for Basic and Frontier Research (112102210005, 112300410095) and the Natural Science Foundation of Henan Educational Committee (2010A150013) and the Foundation for Key Young Teachers of Henan Normal University.

References

1. L.A. Estroff, *Chem. Rev.* **108**, 4329 (2008)
2. J. Aizenberg, J.C. Weaver, M.S. Thanawala, V.C. Sundar, D.E. Morse, P. Fratzl, *Science* **309**, 275 (2005)
3. M.D. Hollingsworth, *Science* **326**, 1194 (2009)
4. H. Imai, *Top. Curr. Chem.* **270**, 43 (2006)
5. C. Robinson, S. Connell, J. Kirkham, R. Shore, A. Smith, *J. Mater. Chem.* **14**, 2242 (2004)
6. M. Sumper, E. Brunner, *Adv. Funct. Mater.* **16**, 17 (2006)
7. Z. Xie, M. Swain, P. Munroe, M. Hoffman, *Biomaterials* **29**, 2697 (2008)
8. A.-W. Xu, Y. Ma, H. Colfen, *J. Mater. Chem.* **17**, 415 (2007)
9. Y. Guo, J. Wang, L. Yang, J. Zhang, K. Jiang, W. Li, L. Wang, L. Jiang, *CrystEngComm* **13**, 5045 (2011)
10. Y. Guo, J. Zhang, L. Yang, H. Wang, F. Wang, Z. Zheng, *Chem. Commun.* **46**, 3493 (2010)
11. F. Wang, Y. Guo, H. Wang, L. Yang, K. Wang, X. Ma, W. Yao, H. Zhang, *CrystEngComm* **13**, 5634 (2011)
12. S. Xiong, B. Xi, C. Wang, G. Zou, L. Fei, W. Wang, Y. Qian, *Chem. Eur. J.* **13**, 3076 (2007)
13. W.-T. Yao, S.-H. Yu, S.-J. Liu, J.-P. Chen, X.-M. Liu, F.-Q. Li, *J. Phys. Chem. B* **110**, 11704 (2006)
14. G.B. Cai, G.X. Zhao, X.K. Wang, S.H. Yu, *J. Phys. Chem. C* **114**, 12948 (2010)
15. X. Ma, H. Chen, L. Yang, K. Wang, Y. Guo, L. Yuan, *Angew. Chem. Int. Ed.* **50**, 7414 (2011)
16. F. Manoli, J. Kanakis, P. Malkaj, E. Dalas, *J. Cryst. Growth* **236**, 363 (2002)
17. H. Tong, W. Ma, L. Wang, P. Wan, J. Hu, L. Cao, *Biomaterials* **24**, 3923 (2004)
18. A.-J. Xie, Y.-H. Shen, C.-Y. Zhang, Z.-W. Yuan, X.-M. Zhu, Y.-M. Yang, *J. Cryst. Growth* **285**, 436 (2005)
19. Y. Guo, L. Wang, L. Yang, J. Zhang, L. Jiang, X. Ma, *Mater. Lett.* **65**, 486 (2011)
20. Y. Guo, L. Jiang, L. Wang, X. Shi, Q. Fang, L. Yang, F. Dong, C. Shan, *Mater. Lett.* **74**, 26 (2012)
21. G. Falini, S. Albeck, S. Weiner, L. Addadi, *Science* **271**, 67 (1996)
22. Q. Shen, L.C. Wang, Y.P. Huang, J.L. Sun, H.H. Wang, Y. Zhou, D.J. Wang, *J. Phys. Chem. B* **110**, 23148 (2006)